Nanotechnology **18** (2007) 424003 (5pp) doi:10.1088/0957-4484/18/42/424003

Carbonyl mediated conductance through metal bound peptides: a computational study

Trilisa M Perrine and Barry D Dunietz[1]

The University of Michigan, Ann Arbor, MI 48109, USA

E-mail: tperrine@umich.edu and bdunietz@umich.edu

Received 23 March 2007, in final form 25 May 2007
Published 13 September 2007
Online at stacks.iop.org/Nano/18/424003

Abstract
Large increases in the conductance of peptides upon binding to metal ions have recently been reported experimentally. The mechanism of the conductance switching is examined computationally. It is suggested that oxidation of the metal ion occurs after binding to the peptide. This is caused by the bias potential placed across the metal–peptide complex. A combination of configurational changes, metal ion involvement and interactions between carbonyl group oxygen atoms and the gold leads are all shown to be necessary for the large improvement in the conductance seen experimentally. Differences in the molecular orbitals of the nickel and copper complexes are noted and serve to explain the variation of the improvement in conductance upon binding to either a nickel or copper ion.

1. Introduction

The unique ability of molecules to recognize and selectively bind to other molecules or ions is integral to many biological systems and processes. When selective binding is accompanied by a measurable change in current or conductance, these recognition mechanisms have numerous potential uses. The conductance switching can be utilized as a chemical sensor for the binding substance [1, 2], and sensing has likewise been accomplished through other aggregate properties [3–6]. The possibility of *single molecule* switches provided by this mechanism is also of vital importance to the field of molecular electronics.

Recent experimental work has reported that single peptide molecules between two gold leads display a significant increase in conductance when bound to metal ions [7]. The conductance of several amino acid sequences was measured with and without the presence of copper and nickel ions. Only the longest amino acid chain, cysteamine–glycine–glycine–cysteine, shows a substantial increase in the conductance upon binding to metal ions. A ratio of 320 is reported between the conductance of the peptide molecule and the peptide bound to a copper ion, and a ratio of 120 is seen between the peptide and the nickel complex. The conductance of the other peptides was not nearly as improved by the complexation to the metal ions. The substantial improvement in the conductance through the long peptide molecule was attributed to the significant conformational change, as well as the additional transmission pathway through the metal ion. In this work, computations are reported which clarify the mechanism of this switching behaviour by further elucidating the chemistry involved in the devices.

2. Computational details

All geometry and electronic structure calculations are performed using density functional theory implemented by QChem 3.0 [8]; the B3LYP [9, 10] functional and the LANL2DZ [11] basis set are utilized. Optimized geometries for the molecules with one gold atom bonded to each sulfur atom are first obtained. Subsequent single point computations are performed with STM tips attached to the gold atoms bonded to each thiol terminus to produce single point energies, overlap matrices and Fock matrices. We follow the scattering based picture of molecular conductance (Landauer formalism) [12–14] based on the Green's function (GF) formalism to calculate the electronic transmission, as described in detail by others [15–21]. These calculations

[1] Author to whom any correspondence should be addressed.

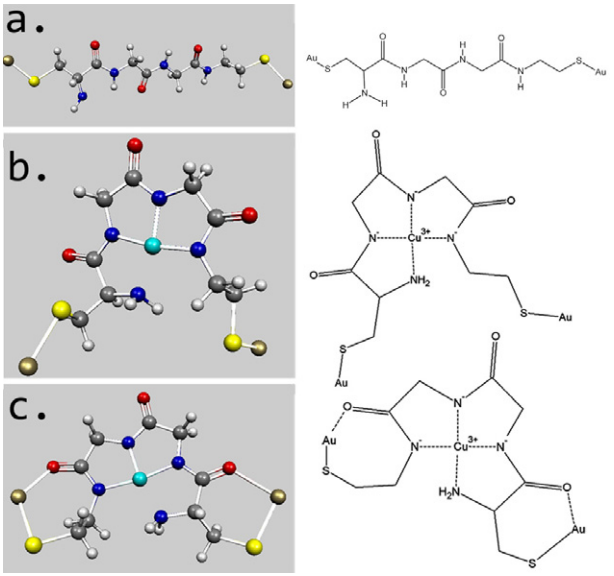

Figure 1. (a) Au–CaGGC–Au, (b) Au–Cu^{3+}–CaGGC–Au with single contacts and (c) Au–Cu^{3+}–CaGGC–Au with ring structures at each end. 1a, 1b and 1c, throughout the text, refer to the corresponding molecular models as shown in this figure.

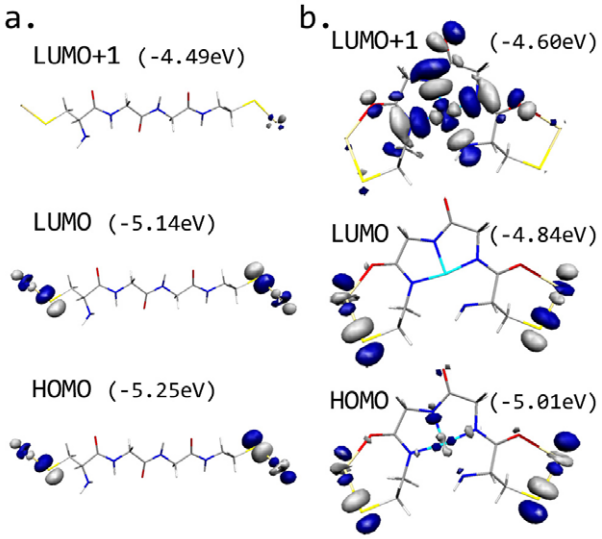

Figure 2. Molecular orbitals of 1a and 1c which lie near E_f of gold. (a) HOMO, LUMO and LUMO + 1 of 1a, and (b) HOMO, LUMO and LUMO + 1 of 1c. The HOMO-1 (not shown) of 1a and 1c has energies of −5.52 and −5.33 eV, respectively, and is localized on one of the Au–S bonds. (All orbitals are drawn with the same isosurface. Only one gold atom is pictured; however, the orbitals are computed with a STM tip attached to the single gold atom shown.)

include a representation of the semi-infinite bulk by efficiently solving a tight-binding (TB) model of the bulk at every energy, where the surface and bulk GFs are solved for iteratively and simultaneously [22–24]. The TB parameters are extracted from the electronic structure calculations described above.

3. Results and discussion

The interesting switching behaviour is experimentally seen for cysteamine–glycine–glycine–cysteine (CaGGC); therefore, CaGGC and its complexes are the primary focus of this computational study. The optimized geometry of CaGGC with one gold atom on each side of the molecule (figure 1a) has a highest occupied molecular orbital (HOMO) at an energy of −5.85 eV and a lowest unoccupied molecular orbital (LUMO) at −4.68 eV. The HOMO and LUMO are relatively close in energy to the Fermi energy (E_f) of gold (−5.2 eV), which allows for transmission through the CaGGC molecule. Single point computations of CaGGC with gold STM tips attached at each end give HOMO and LUMO energies of −5.25 and −5.14 eV, respectively. As seen in figure 2a, the HOMO and LUMO of CaGGC are localized orbitals along both S–Au bonds. Molecular electronic densities are known to allow transmission of an electron if they are delocalized across the molecule. Therefore, the bare peptide is established to be a relatively poor conductor, as confirmed by the experimental observations [7].

The metal–peptide complexes are prepared experimentally by the addition of Cu^{2+} or Ni^{2+} ions to the peptide solution. To facilitate the complexation, this is performed at a pH of 8 to deprotonate the peptide's nitrogen sites. During the conductance and current measurements, a voltage is placed across the molecule through the connection to the gold leads [7]. Preparations of Cu^{2+} and Ni^{2+} peptide complexes are well known; however, the complexes can also be oxidized by either an oxidizing agent or an electrochemical process to form the Cu^{3+} and Ni^{3+} complexes. Remarkably, Cu^{3+} and Ni^{3+} peptide complexes are relatively stable in aqueous solution and in slightly basic solutions, with half-lives on the order of hours to weeks [25–31]. The Cu^{3+}–peptide complexes are known to have square planar coordination due to the d^8 electron configuration of the Cu^{3+} ion, and the low-spin state is preferred. The redox potential of the $Cu^{3+} + e^- \rightleftharpoons Cu^{2+}$ reaction is 1.57 V [32]. However, the Cu(III)–Cu(II) potentials vary substantially (in the range of 0.45–1.02 V) for complexes with different peptide ligands [33]. The Ni(III)–Ni(II) potential is less sensitive to the specific peptide ligand, with values from 0.8 to 0.9 V [34].

In order to measure the current through the metal–peptide complexes, a potential is applied directly to the molecule through the gold leads. During the course of the experiment, this bias potential is swept between −0.8 and 0.8 V. Due to the relatively low oxidation potentials for the metal–peptide complexes, it is suggested that this bias potential oxidizes the metal ion. This leaves the copper(III) or nickel(III) ion bound to the peptide, instead of the presumed copper(II) or nickel(II) ions. Thus, we explore the electronic structure of the Cu^{3+} and Ni^{3+} complexes, in addition to the Cu^{2+} and Ni^{2+} complexes. For completeness, the unusual oxidation state +4 and +1 ion complexes have also been computed.

Geometry optimizations of the metal ion–peptide systems show multiple stable geometries. Two extreme geometries for each complex are compared as model systems. One geometry has no interaction between the carbonyl group and the gold atom on either end of the molecule (figure 1b). The other has a pseudo-ring structure at each contact involving the thiol–Au bond as well as an interaction between the gold atom and a nearby carbonyl group (figure 1c). The Cu^{3+}–peptide

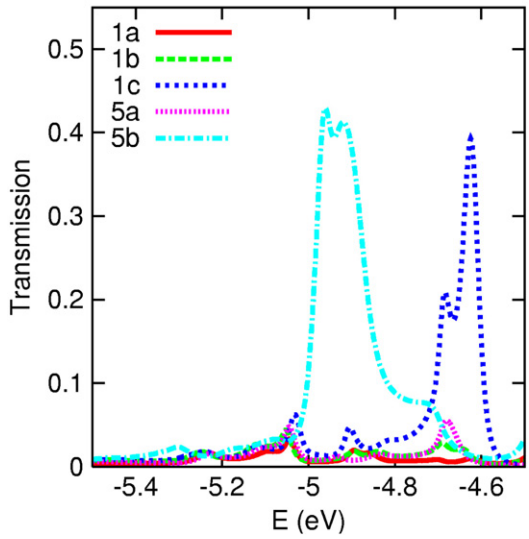

Figure 3. Transmission (arbitrary units) of 1a, 1b, 1c, 5a and 5b.

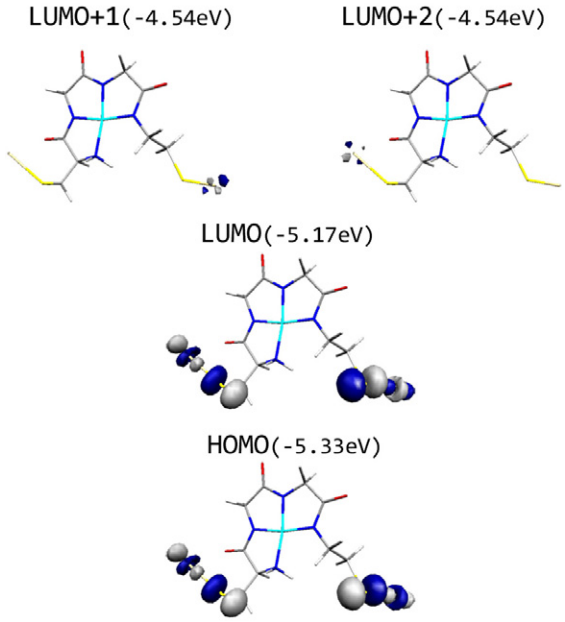

Figure 4. HOMO, LUMO, LUMO + 1 and LUMO + 2 of the Au–Cu^{3+}–CaGGC–Au system with no interaction between the carbonyl group and the gold atom (1b). (All orbitals are drawn with the same isosurface. Only one gold atom is pictured; however, the orbitals are computed with an STM tip attached to the single gold atom shown.)

geometries are shown in figures 1b and 1c, respectively. The nickel and other copper ion complex geometries are very similar. The 1b and 1c Cu^{3+}–peptide configurations with one gold at each terminal differ by only 0.02 eV, with the 1b arrangement being lower in energy than in 1c.

An examination of the molecular orbitals of the above systems reveals that all of the complexes with metal ions of charge +1, +2 or +4 have a HOMO and LUMO which have energies far from the E_f of gold. This misalignment of E_f with the HOMO makes the +1, +2, and +4 ion complexes poor candidates for conduction. The Cu^{3+} and Ni^{3+} peptide complexes, however, have HOMOs and LUMOs which align relatively well with the Fermi level of the leads. We therefore concentrate below on the conduction of the +3 ion systems.

The transmission functions of several CaGGC complexes are shown in figure 3. The peptide without a metal bound to it (1a) is seen to have very low transmission as expected from the previous discussion of the localization of the HOMO and LUMO. The metal bound system with no interaction between the carbonyl and the gold surface (1b), however, has only slightly better transmission than that of 1a.

An analysis of the electronic density is useful to explain the negligible improvement in the transmission of 1b over that of 1a. This is accomplished by focusing on the HOMO and low-lying unoccupied orbitals of 1b. In figure 4 the HOMO, LUMO, LUMO + 1 and LUMO + 2 of 1b are shown. As in 1a, the orbitals which lie near E_f for 1b are localized along the Au–S bonds, and no effective pathway for transmission is evident.

The transmission through the molecular configuration which involves an interaction between the gold leads and the carbonyl groups 1c, is significantly improved over that of 1a and 1b. This arises from the available efficient transmission pathway through the metal ion and the carbonyls. The molecular orbitals of 1c, near E_f, are shown in figure 2b. Similar to the HOMO and LUMO of 1a and 1b, the HOMO and LUMO of 1c have a substantial density along the Au–S bonds. However, these orbitals have density along the Au–O (carbonyl) interactions as well. The HOMO of 1c also has some density on the metal ion itself. The transmission through the HOMO and LUMO is seen as small peaks in the transmission plot (figure 3) at about −5.0 and −4.9 eV, respectively. The most prominent peak in the transmission for 1c, however, occurs at a higher energy (approximately −4.6 eV), and is due to the second virtual orbital, LUMO + 1. This orbital is delocalized over the peptide–Cu^{3+} portion of the system, and the Au–O interaction is more dominant than the Au–S bond for this orbital. This interaction between the O and Au atoms appears to yield a more efficient pathway from one gold atom to the other through the metal ion, allowing for the larger transmission through the molecule seen in figure 3.

To further explore the conductance switching mechanism two model systems are utilized. First, a model which retains the ring structures defined by the 1c geometry is used; however, the Cu^{3+} is removed and each of the deprotonated nitrogen atoms is re-protonated (figure 5a). This is an artificial model, since, upon protonation, the molecule will unfold and return to a geometry similar to 1a. However, this model allows a separation of the effect of the simple configurational change upon binding to the metal from the effect of the metal centre itself. Transmission through this model system, as shown in figure 3, is only marginally better than that through the extended linear geometry (1a). Therefore, the configurational change which takes place upon binding to the metal cannot *solely* explain the substantial jump in the conductance which is experimentally observed.

Next, a second model system is used to study the effect of the carbonyl–Au interaction on the transmission. Here again, the basic geometry of 1c is used, but in the model system

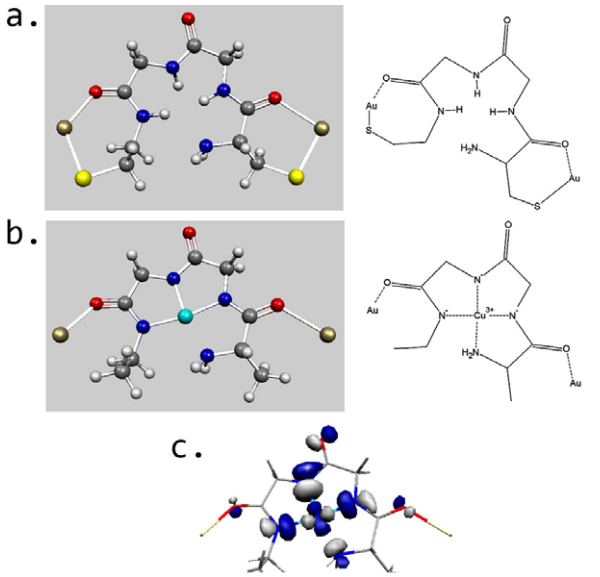

Figure 5. Model systems where the geometry of 1c is altered by (a) removing the Cu^{3+} ion and reprotonating each N atom and (b) replacing the S atoms with H atoms. (c) The LUMO (−4.84 eV) of 5b. 5a and 5b, throughout the text, refer to the corresponding molecular models as shown in the figure.

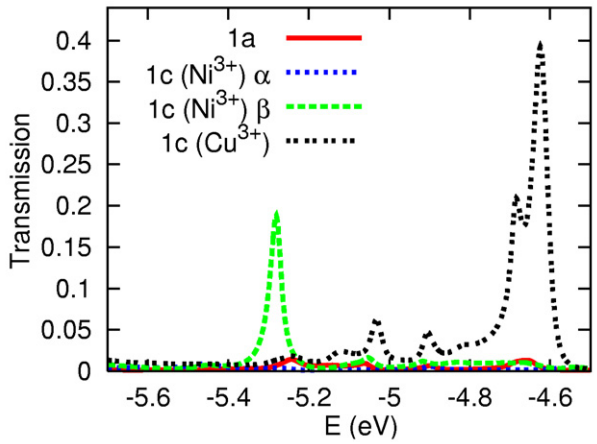

Figure 6. Transmission (arbitrary units) of 1a, 1c with Ni^{3+}, and 1c with Cu^{3+}. The transmission of 1c with Ni^{3+} is shown as separate α and β channels.

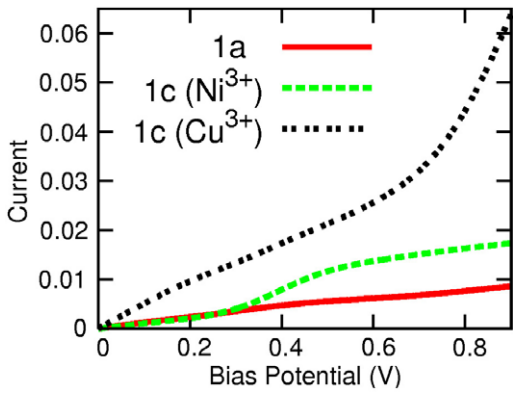

Figure 7. Current (27.211 ∗ au) of 1a, 1c with Ni^{3+}, and 1c with Cu^{3+}.

the sulfur atom at each end is replaced with a hydrogen atom (figure 5b). This model has no Au–S bonds, and thus the only path for transmission is through the Au–O interaction. The transmission through 5b (shown in figure 3) is quite large when compared to the transmission of 1a and 1b. In contrast, the overall shape and height of the transmission peaks for 5b are quite similar to those for the highly conducting geometry of 1c. The locations of the peaks are shifted, however, and the largest peak is closer to the Fermi energy of the leads for 5b. The similarity in the large peaks is explained by the molecular orbitals responsible for these high transmission peaks. As previously discussed, for 1c the LUMO + 1 is responsible for the large peak in the transmission. For 5b, the transmission peak is attributed to the LUMO of the system at −4.84 eV, which is shown in figure 5c. The shape and span of the LUMO + 1 of 1c closely resemble that of the LUMO of 5b. The observed shift in the location (and orbital energy) of the transmission peak towards E_f upon removal of the thiol groups highlights the somewhat destructive effect of the thiol–Au bond on the conductance.

Experimentally the nickel and copper complexes each show improved conductance over the bare peptide; however, the improvement of the copper–CaGGC complex is significantly better than that of the nickel–CaGGC system [7]. The same trend is displayed by the computational results. Figures 6 and 7 show the computed transmission and current for the bare peptide (1a), and the two metal–peptide complexes which involve the interaction between the carbonyl groups and the gold leads at each terminal. The ground state of Ni^{3+}–CaGGC is a doublet, in contrast to CaGGC and Cu^{3+}–CaGGC which are both singlets. The α and β transmission channels are thus shown separately for Ni^{3+}–CaGGC in figure 6, while the two current values have been summed in figure 7. The β channel is seen to dominate the transmission for Ni^{3+}–CaGGC, with a peak in the transmission around −5.3 eV. There are two β molecular orbitals near that energy, and both involve some density on the metal ion, the carbonyl groups and the gold terminals. In contrast to the Cu^{3+} system, the molecular orbitals responsible for transmission through Ni^{3+}–CaGGC are occupied orbitals (HOMO and HOMO-1). This is a surprising result, since the Cu^{3+} ion has one more electron than the Ni^{3+} ion. The LUMO + 1 orbital responsible for transmission in the Cu^{3+}–CaGGC system is primarily of σ^* character on the metal–peptide portion of the system; however, the metal–peptide portion of the transmitting orbital for Ni^{3+}–CaGGC is essentially a π^* molecular orbital oriented perpendicular to the transmission pathway. These differences between relevant molecular orbitals in the copper(III) and nickel(III) systems can explain the significant difference in the switching capacity of the two metal complexes. The current for Cu^{3+}–CaGGC is substantially better than that of Ni^{3+}–CaGGC as seen in figure 7. These differences in response can ultimately be utilized to differentiate between a variety of metals.

4. Conclusion

Large jumps in conductance are seen experimentally for CaGGC upon binding to nickel and copper ions. The conductance increase is significantly larger for the copper complex than for the nickel complex [7]. Due to the relatively small Cu(III)/Cu(II) and Ni(III)/Ni(II) potentials and the experimental conditions, Cu(III)–peptide and Ni(III)–peptide complexes are likely to be produced. We also find that these complexes (Cu^{3+}–CaGGC and Ni^{3+}–CaGGC) have a better alignment of their electronic densities with the Fermi energy of gold leads than the Cu^{2+} and Ni^{2+} complexes. The molecular orbitals near E_f differ in energy and shape for the Cu(III)–peptide and Ni(III)–peptide systems. This accounts for the variation in the response of the conductance upon binding to the different metal ions.

Simple configurational rearrangement is not adequate to explain the large change in the conductance seen in experiments between the peptide and the peptide–metal complexes, nor is the metal binding to the peptide enough to increase the conductance significantly, as the transmission through 1b shows little improvement over 1a. We also note that while the carbonyl–Au interactions are found to be important in the high transmission configurations, they are not, in themselves, *sufficient* to increase the transmission. This is evident, since the transmission seen for 5a is nearly identical to that of 1a.

The similarities in the orbitals and transmission peaks of Cu^{3+}–CaGGC with carbonyl–Au interactions (1c) and the same system without any thiol–Au bonds (5b) suggest that the pathway through the Au–O interaction is the primary mechanism by which the conductance through the peptide is increased upon binding to the metal ions.

Therefore, the model calculations show that the conformational change, the metal ion centre and the carbonyl–gold interaction are all necessary for the large increase in conduction to occur upon binding of the metal ion to the peptide. Conversely, it is seen that the Au–S bonds are not only unnecessary for the transmission, but are, in fact, detrimental to the transmission through the molecular system. While the Au–S bonds play an integral part in the formation of the gold–molecule–gold systems, they raise the energy of the highly conducting orbital, and push it farther from the Fermi energy of the gold leads.

We have provided in this paper, through state-of-the-art computational methods, an atomic scale insight into recent striking experimental findings concerning peptide–metal ion conductance. Further computational work is pursued to explore the two primary aspects of the described conductance mechanism. This entails a focus on the interplay of the two surface binding types, including the carbonyl and the more ubiquitous sulfur bond. The second aspect involves additional exploration of an array of metal–peptide complexation systems, which can be used as a guide for performing additional interesting experiments.

Acknowledgments

BDD acknowledges the University of Michigan for financial support and Prof. Mark Banaszak-Holl for useful discussions.

References

[1] Yang W R, Chow E, Willett G D, Hibbert D B and Gooding J J 2003 *Analyst* **128** 712
[2] Yang W, Jaramillo D, Gooding J J, Hibbert D B, Zhang R, Willett G D and Fisher K J 2001 *Chem. Commun.* **19** 1982
[3] McQuade D T, Pullen A E and Swager T M 2000 *Chem. Rev.* **100** 2537
[4] Ricco A J, Crooks R M and Osbourn G C 1998 *Acc. Chem. Res.* **31** 289
[5] Thundat T, Finot E, Hu Z, Ritchie R H, Wu G and Majumdar A 2000 *Appl. Phys. Lett.* **77** 4061
[6] Zhang H W, Boussaad S, Ly N and Tao N J 2004 *Appl. Phys. Lett.* **84** 133
[7] Xiao X, Xu B and Tao N J 2004 *Angew. Chem. Int. Edn* **43** 6148
[8] Shao Y *et al* 2006 *Phys. Chem. Chem. Phys.* **27** 3172
[9] Becke A D 1993 *J. Chem. Phys.* **98** 1372
[10] Becke A D 1993 *J. Chem. Phys.* **98** 5648
[11] Hay J P and Wadt W R 1985 *J. Chem. Phys.* **82** 299
[12] Landauer R 1970 *Phil. Mag.* **21** 863
[13] Bagwell P F and Orlando T P 1989 *Phys. Rev.* B **40** 1456
[14] Imry Y and Landauer R 1999 *Rev. Mod. Phys.* **71** S306
[15] Samanta M P, Tian W, Datta S, Henderson J I and Kubiak C P 1996 *Phys. Rev.* B **53** R7626
[16] Tian W D, Datta S, Hong S H, Reifenberger R, Henderson J I and Kubiak C P 1998 *J. Chem. Phys.* **109** 2874
[17] Mujica V, Nitzan A, Mao Y, Davis W, Kemp M, Roitberg A and Ratner M A 1999 *Adv. Chem. Phys.* **107** 403
[18] Xue Y, Datta S and Ratner M A 2001 *J. Chem. Phys.* **115** 4292
[19] Baer R and Neuhauser D 2002 *J. Am. Chem. Soc.* **124** 4200
[20] Liu C, Walter D, Neuhauser D and Baer R 2003 *J. Am. Chem. Soc.* **125** 13936
[21] Yaliraki S N, Roitberg A E, Gonzalez C, Mujica V and Ratner M A 1999 *J. Chem. Phys.* **111** 6997
[22] Lopez Sancho M P, Lopez Sancho J M L and Rubio J 1985 *J. Phys. F: Met. Phys.* **15** 851
[23] Nardelli M B 1999 *Phys. Rev.* B **60** 7828
[24] Prociuk A, Van Kuiken B and Dunietz B D 2006 *J. Chem. Phys.* **125** 204717
[25] Margerum D W, Chellappa K L, Bossu F P and Burce G L 1975 *J. Am. Chem. Soc.* **97** 6894
[26] Youngblood M P and Margerum D W 1980 *Inorg. Chem.* **19** 3068
[27] Raycheba J T and Margerum D W 1981 *Inorg. Chem.* **20** 45
[28] Koval C A and Margerum D W 1981 *Inorg. Chem.* **20** 2311
[29] Rybka J S and Margerum D W 1981 *Inorg. Chem.* **20** 1453
[30] Owens G D and Margerum D W 1981 *Inorg. Chem.* **20** 1446
[31] Neubacker T A, Kirksey S T Jr, Chellappa K L and Margerum D W 1979 *Inorg. Chem.* **18** 444
[32] Popova T V and Aksenova N V 2003 *Russ. J. Coord. Chem.* **29** 743
[33] Cotton F A, Wilkinson G, Murillo C A and Bochmann M 2003 *Advanced Inorganic Chemistry* 6th edn (New York: Wiley)
[34] Bossu F P and Margerum D W 1977 *Inorg. Chem.* **16** 1210